AFRL-RV-PS-
TR-2016-0046

AFRL-RV-PS-
TR-2016-0046

PHYSICALLY PROTECTED SPREAD SPECTRUM COMMUNICATIONS

Hyuck M. Kwon

Wichita State University
1845 N. Fairmount Ave.
Wichita, Kansas 67260

14 Apr 2016

Final Report

APPROVED FOR PUBLIC RELEASE; DISTRIBUTION IS UNLIMITED.

AIR FORCE RESEARCH LABORATORY
Space Vehicles Directorate
3550 Aberdeen Ave SE
AIR FORCE MATERIEL COMMAND
KIRTLAND AIR FORCE BASE, NM 87117-5776

DTIC COPY

NOTICE AND SIGNATURE PAGE

AFRL-RV-PS-TR-2016-0046 HAS BEEN REVIEWED AND IS APPROVED FOR PUBLICATION IN ACCORDANCE WITH ASSIGNED DISTRIBUTION STATEMENT.

//SIGNED//

KHANH PHAM
Program Manager

//SIGNED//

PAUL D. LEVAN, Ph.D.
Technical Advisor, Space Based Advanced Sensing and Protection

//SIGNED//

JOHN BEAUCHEMIN
Chief Engineer, Spacecraft Technology Division
Space Vehicles Directorate

REPORT DOCUMENTATION PAGE	*Form Approved* *OMB No. 0704-0188*

1. REPORT DATE *(DD-MM-YY)*	**2. REPORT TYPE**	**3. DATES COVERED** *(From - To)*
14-04-2016	Final Report	11 Dec 2014 – 11 Mar 2016

4. TITLE AND SUBTITLE
Physically Protected Spread Spectrum Communications

5a. CONTRACT NUMBER
FA9453-15-1-0308

5b. GRANT NUMBER

5c. PROGRAM ELEMENT NUMBER
62601F

6. AUTHOR(S)

Hyuck M. Kwon

5d. PROJECT NUMBER
8809

5e. TASK NUMBER
PPM00019106

5f. WORK UNIT NUMBER
EF123296

7. PERFORMING ORGANIZATION NAME(S) AND ADDRESS(ES)

Wichita State University
1845 N. Fairmount Ave.
Wichita, Kansas 67260

8. PERFORMING ORGANIZATION REPORT NUMBER

R51249

9. SPONSORING / MONITORING AGENCY NAME(S) AND ADDRESS(ES)
Air Force Research Laboratory
Space Vehicles Directorate
3550 Aberdeen Ave., SE
Kirtland AFB, NM 87117-5776

10. SPONSOR/MONITOR'S ACRONYM(S)
AFRL/RVSW

11. SPONSOR/MONITOR'S REPORT NUMBER(S)
AFRL-RV-PS-TR-2016-0046

12. DISTRIBUTION / AVAILABILITY STATEMENT
Approved for public release; distribution is unlimited.

13. SUPPLEMENTARY NOTES

14. ABSTRACT
This report considers a coherent (instead of noncoherent) modulation such as an M-ary phase-shift keying (MPSK) and M-ary quadrature amplitude-shift keying (MQAM) for a slow frequency hopping (FH) spread spectrum (SS) system because, recently, coherent modulation has been the candidate for a future satellite FH waveform. Then, the PI found an exact symbol error rate (SER) expression for the FH system under partial-band tone jamming (PBTJ) and Rician fading environments through analysis. In addition, the PI studied the optimal weighting coefficients for each hop interval to minimize the SER. Furthermore, the PI derived an implicit expression of the optimal PBTJ fraction ratio, which maximizes the SER of the FH system and compares the analytical results with the numerical results for verification. The results shown here can be useful for the design of future efficient game theoretic FH satellite and mobile communications systems when a coherent FH modulation is employed under severe fading as well as severe PBTJ environments.

15. SUBJECT TERMS
Frequency hopping, spread spectrum, coherent modulation, Rician fading, partial band tone jamming, symbol error rate

16. SECURITY CLASSIFICATION OF:			**17. LIMITATION OF ABSTRACT**	**18. NUMBER OF PAGES**	**19a. NAME OF RESPONSIBLE PERSON** Khanh Pham
a. REPORT Unclassified	**b. ABSTRACT** Unclassified	**c. THIS PAGE** Unclassified	Unlimited	46	**19b. TELEPHONE NUMBER** *(include area code)*

Standard Form 298 (Rev. 8-98)
Prescribed by ANSI Std. 239.18

(This page intentionally left blank)

Table of Contents

List of Figures

ACKNOWLEDGEMENTS

This material is based on research sponsored by Air Force Research Laboratory under agreement number FA9453-13-1-0292. The U.S. Government is authorized to reproduce and distribute reprints for Governmental purposes notwithstanding any copyright notation thereon.

DISCLAIMER

The views and conclusions contained herein are those of the authors and should not be interpreted as necessarily representing the official policies or endorsements, either expressed or implied, of Air Force Research Laboratory or the U.S. Government.

Abstract

This report considers a coherent (instead of noncoherent) modulation such as an M-ary phase-shift keying (MPSK) and M-ary quadrature amplitude-shift keying (MQAM) for a slow frequency hopping (FH) spread spectrum (SS) system because, recently, coherent modulation has been the candidate for a future satellite FH waveform [19]-[22]. Then, the PI found an exact symbol error rate (SER) expression for the FH system under partial-band tone jamming (PBTJ) and Rician fading environments through analysis. In addition, the PI studied the optimal weighting coefficients for each hop interval to minimize the SER. Furthermore, the PI derived an implicit expression of the optimal PBTJ fraction ratio, which maximizes the SER of the FH system and compares the analytical results with the numerical results for verification. The results shown here can be useful for the design of future efficient game theoretic FH satellite and mobile communications systems when a coherent FH modulation is employed under severe fading as well as severe PBTJ environments.

Index Terms—Frequency hopping, spread spectrum, coherent modulation, Rician fading, partial band tone jamming, and symbol error rate.

1. SUMMARY

The PI achieved the five objectives stated in the original proposal during the period from December 15, 2014, to December 14, 2015, by doing the following:

- Conducted research into an anti-interference physical-layer strategy that leverages spread spectrum (SS) communications to be more robust, reliable, sustainable, and energy-efficient than existing ones.
- Determined whether the proposed novel approach is feasible in a SS satellite communications system by modeling a system controller (SC), a satellite transponder, and a terminal, as a transmitter, an amplify-and-forward (AF) relay, and a receiver, respectively.
- Proved the proposed concept through simulation.
- Evaluated the merits and disadvantages of the proposed strategy by doing the following: (1) comparing the bit error rate (BER) performance with those of existing schemes in the presence of multiple access (MA) interference signals, (2) computing the computational complexities, and (3) addressing feasibility and compatibility of the proposed scheme with existing schemes.
- Recomputed and replotted all numerical results in the performance report and corrected all programing errors. Extended the obtained results from a single input single output (SISO) communication system to a single input multiple output (SIMO) system to achieve beamforming (BF) during the research period from September 2, 2015, to December 15, 2015.

These achievements have led to the application for a U.S. patent disclosure: Hyuck M. Kwon and Khanh Pham, "System and Method for Generating Exact Symbol Error Rates of Frequency-

Hopped Signals," U.S. Nonprovisional Patent Application No. 14/926,746, Attorney Docket No. 47674, filed on October 29, 2015. These achievements are summarized in this final report, and the content will be disclosed through peer-reviewed journal and conference proceedings publications.

In the PI's performance report written on September 1, 2015, the PI requested not to pursue the following objectives, as stated in the original proposal, because a frequency hopping spread spectrum (FHSS) system with coherent modulation has recently been the candidate for a future protected tactical satellite waveform instead of the direct-sequence code-division-multiple-access (DS-CDMA) spread spectrum (SS) waveform:

- To investigate a novel, unique, simple, and anti-interference approach for SS systems so that the proposed research would be applicable to a general communication system, and also to design a pair of channel state information (CSI)-dependent time-domain beam-forming (TDBF) vectors that can be used at a transmitter and a receiver (called pre- and post-coding vectors) for an FHSS system.
- To investigate the pseudo-noise (PN) sequence time synchronization performance for a DS-CDMA SS system, using a pair of CSI-dependent PN spreading/despreading sequences that are obtained with the proposed research principle.

The PI continued to investigate more interesting and practical problems after his 2015 Air Force Summer Faculty Fellowship Program (AF SFFP) related to future FHSS satellite communications systems, such as robust FH pattern designs with higher energy efficiency against intentional jamming signals, i.e., a lower SER at a given bit-energy-to-noise power spectral density ratio than existing FH patterns. The achievement has also led to another application for a U.S. patent disclosure: Hyuck M. Kwon, Matthew Hannon, and Khanh Pham, “System and Method for Channel Statistics Dependent Frequency Hopping,” US Nonprovisional Patent Application. No. 14/926,833, Attorney Docket 47675, Filed on October 29, 2015.

2. INTRODUCTION

In today's fast-paced world, connectivity is of prime importance to everyone. It is not only necessary to be connected to everyone, but faster access of data through the cloud or any other medium is imperative. Various techniques have been proven to deploy a fast and efficient network. Technologies such as wideband-code division multiple access (W-CDMA), high-speed downlink packet access (HSDPA), long-term evolution (LTE), and LTE-Advanced have been popular for high-speed mobile communications [1]-[3]. But the question to ask is whether or not the connection to the network or other users would be secure.

Due to various malicious activities, such as jamming and eavesdropping, it is vital to have an error-free and secure transmission. Eavesdropping is a very serious issue since the user's privacy can be in jeopardy and result in an enormous loss of information. One of the most effective jamming attacks is partial-band tone jamming (PBTJ) or partial-band noise jamming (PBNJ) [4], [5]. Both are similar, and the PBTJ is more effective but can be exposed to friendly users more than PBNJ. This paper considers PBTJ, which reduces system symbol error rate (SER) performance and degrades throughput efficiency by reducing the effective signal-to-noise ratio (SNR) of the user. A successful solution to this issue can be addressed by moving into the 2.4 GHz frequency band, where spread spectrum communication operates [6]-[8]. Spread spectrum communication is a vital technique for establishing secure connections among various applications including the military as well as commercial mobile communications [9].

Some of the most commonly used military radios that make use of frequency hopping belong to the joint tactical information distribution system (JTIDS), multifunctional information distribution system (MIDS), and single-channel ground and airborne radio system (SINCGARS) [10]-[12]. The preference of operation is given to frequency hopping (FH) spread spectrum communication because it is difficult to intercept messages due to the presence of a pseudo random sequence key generation in transmission security (TRANSEC) in every message [13].

Because of this advantage and because the future military satellite waveform considers a slow FH, this paper studies slow FH communication in the presence of a PBTJ jamming scenario. Here, a slow FH means multiple symbols transmitted per hop. Again, the existing FH pattern design employs both a hopping keystream and a time permutation keystream for resistance to jamming and detection. The entire hopping spectrum is uniformly occupied over a large number of hops. Hence, we assume a random FH pattern, which is good, in order to cause a low probability of detection. However, the probability of a hit by a single-tone jammer for the random FH pattern is high such as $1/N_f$, where N_f denotes the total number of frequency positions in the entire hopping spectrum. Once a desired narrow band signal is hit by a tone jammer with sufficient jamming power, half of the symbols in the hop are likely to be in error for a binary modulation. If a jammer has sufficient power, then it can generate multiple tones instead of a single tone. This is why we consider PBTJ and want to determine the optimum (i.e., the worst case) PBTJ fraction ratio for a given jamming power constraint.

Between late 1970 and early 1990, FH communications systems under various types of jamming have been studied [14]-[18], considering noncoherent modulations such as M-ary frequency-shift keying (MFSK) and M-ary differential phase-shift keying (MDPSK). For example, in [17], the authors presented a method for calculating MDPSK error probability in PBTJ and additive white Gaussian noise (AWGN). Also, Rician fading was considered. In [18], the author studied fundamental limitations on repeater jamming of frequency-hopping communications. In the literature, the Chernoff upper bound was frequently used for the bit error probability derivation due to the difficulty in getting the exact error probability.

It has been known that a coherent modulation such as an M-ary phase-shift keying (MPSK) is more bandwidth efficient than a noncoherent modulation such as an MFSK. The reason why the coherent modulation such as M-ary phase-shift keying (MPSK) was not employed for the FH system in those days was because of implementation issues, such as a frequency-ringing problem, which occurred whenever a frequency was hopped to a new frequency.

Today, these implementation technologies have improved, and MPSK has been considered for future satellite FH systems to achieve bandwidth efficiency over the noncoherent MFSK modulation [19]-[22]. However, there has not been an exact symbol error rate (SER) analysis of FH/MPSK under PBTJ and Rician fading. This is the main motivation of this paper. This paper presents an exact SER of the FH/MPSK under PBTJ and Rician fading using the moment generation function (MGF) and the Craig's formula [23]-[26]. Numerical SER results of the FH/MPSK under Rician fading and PBTJ are presented. The analysis in this paper can be extended for other coherent modulations such as M-ary quadrature amplitude modulation (MQAM), other mobile fading environments such as Nakami and Rayleigh, and other jamming such as PBNJ without difficulty. Optimal weighting coefficients for each hop interval are also considered. Furthermore, the optimal PBTJ fraction ratio is derived and compared with numerical results.

Before moving to the system model section, we would like to mention an effective alternative robust FH system with noncoherent detection in [9, pp. 545], [27], which shows a performance close to that of a coherent system, even if it employs noncoherent, nonorthogonal continuous-phase frequency-shift keying (CPFSK). This CPFSK FH is practical and useful for future satellite communication systems for the following reasons: (a) it does not require any pilot symbols and reference symbols for coherent phase tracking and channel estimation after every frequency hop;

(b) the probability of interference by PBTJ is lower than that for conventional MFSK due to the compact signal band occupancy; and (c) it shows bit error rate (BER) performance with negligible degradation in SNR, compared to that of a coherent FH system. These advantages of the CPFSK FH in [9], [27] can be provided by employing bit-interleaved coded modulation (BICM), iterative turbo decoding and demodulation, and channel estimation, although it employs noncoherent detection [28].

This current paper can also apply the same principle of BICM to the coherent MPSK FH presented in [19]-[22] and improve the BER significantly, as was done in [9], [27] against fading and jamming with iterative turbo decoding and demodulation, and channel estimation. It is expected that the number of pilot symbol or reference symbols can be significantly reduced from those required for MPSK FH with no BICM, or completely removed, as demonstrated in the coded direct-sequence code division multiple access (DS-CDMA) system study [29]. The current paper focuses on the physical layer design without considering the BICM for the following reasons: (a) it is beyond the scope of this paper; and (b) the BICM structure has not been determined yet for the future MILSATCOM system in [19]-[22]. This task will be performed in the future.

Results in this paper can still be useful for efficient FH satellite and mobile communications system designs when a coherent MPSK FH modulation is employed under severe fading as well as a severe PBTJ environment. Specifically, the numerically obtained results can be useful for the future protected tactical satellite waveform design [19]-[22], which may employ the game theory between desired users and jammers. The game theoretical analysis is not included in this paper because it is beyond the scope of this paper. Also, no error-correction coding is considered, and only uncoded physical layer SER results are presented here. For a given error-correction code, the overall decoded BER performance can be computed using the uncoded SER analysis in this paper, if the coding and modulations are separated.

The rest of the paper is organized as follows: Sections II describes the system model. Then, Section III presents an exact SER expression of the FH/MPSK under the AWGN, PBTJ, and Rician fading. Section IV finds an expression to determine the optimum PBTJ fraction. Section V shows numerical results, and Section VI concludes the paper.

Notations: The upper-bar, e.g., $\overline{X}$, denotes the average value of a random variable X; $E[X]$ also denotes the expectation or average of a random variable X; the bold lower case, e.g., $\boldsymbol{x}$ denotes a vector; $\boldsymbol{x}^T$ denotes the transpose of vector $\boldsymbol{x}$; $\|\boldsymbol{x}\|$ denotes the norm of vector $\boldsymbol{x}$; and $|x|$ denotes the magnitude of a complex number x.

3.0 METHODS, ASSUMPTIONS, AND PROCEDURES

The entire FH spectrum is divided into N_f number of channels operating at frequencies $f_1, \cdots$, and f_{N_f}. All channels are independent of each other and have a hop interval denoted by T_h. One data frame consists of L_h number of time hops. Since a slow frequency hopping is considered, N_s multiple symbols are transmitted per hop. For example, Fig. 1 shows an FH/MPSK of $N_f = 3$ frequency channels, $L_h = 2$ time hops per frame, $N_s = 2$ number of symbols per hop, and $N_u = 2$ number of MA users sharing the entire FH spectrum. Fig. 1 is shown just for an illustration purpose of the FH/MPSK notations, and the practical parameters are different from these.

The transmitted signal for the *k*-th user is denoted by $s_{ij}^{(k)}(t)$, where the superscript *k* denotes the user index, and subscripts *i* and *j* indicate the symbol index and frequency index in a hop, respectively. In Fig. 1, user 1's signals are $s_{11}^{(1)}(t)$ and $s_{21}^{(1)}(t)$ for the hop 1 interval, and $s_{13}^{(1)}(t)$ and $s_{23}^{(1)}(t)$ for the hop 2 interval, and user 2's signals are $s_{13}^{(2)}(t)$ and $s_{23}^{(2)}(t)$ for the hop 1 interval, and $s_{12}^{(2)}(t)$ and $s_{22}^{(2)}(t)$ for the hop 2 interval. Without loss of generality in analysis, consider that user 1 uses frequency f_1 during hop 1. The transmitted MPSK signal by user 1 can be written as

$$s_{11}^{(1)}(t) = Ag(t)cos\left[\frac{2\pi(i-1)}{M}\right]cos[2\pi f_1 t] - Ag(t)sin\left[\frac{2\pi(i-1)}{M}\right]sin[2\pi f_1 t], i = 1, \cdots, M \quad (1)$$

where $0 \leq t \leq T_s$, A is the amplitude of the signal, $g(t)$ is the waveform shaping filter, e.g., a root raised cosine filter (RRC), and i denotes the transmitted symbol out of M possible symbols.

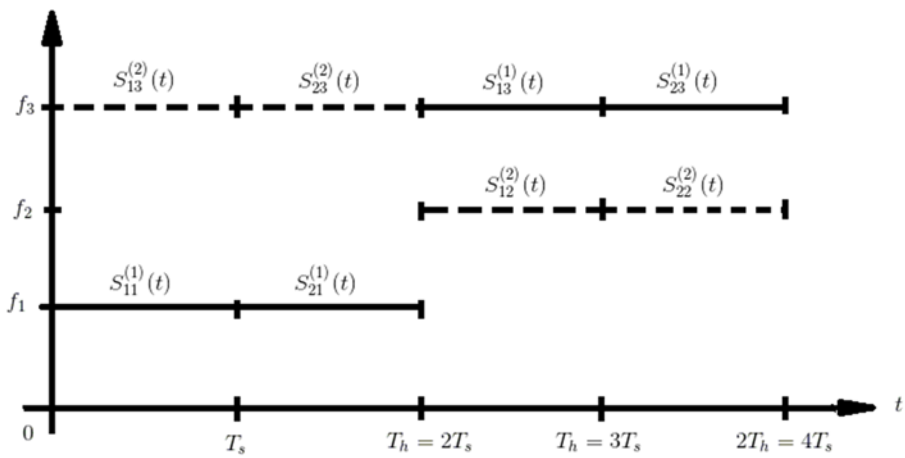

Figure 1. Hopping patterns for $N_u = 2$ users, $N_s = 2$ symbols/hop, $N_f = 3$ frequencies, and $L_h = 2$ time hops per frame.

Rician fading is assumed with channel coefficient $h_1 = |h_1|e^{j\theta_1}$, where $|h_1|$ and θ_1 are the Rician amplitude and the uniformly distributed angle of h_1, respectively [25]. It is also assumed that the transmitter is constantly under attack by PBTJ. The PBTJ signal $j(t)$ during the first symbol, first hop interval ($0 \leq t \leq T_h$) relative to user 1's signal is written as

$$j(t) = \begin{cases} \sqrt{2}A_J cos\left[2\pi f_1 t + \emptyset_J\right] & \text{if user 1's signal is jammed} \\ 0 & \text{else} \end{cases} \quad (2)$$

where A_J is the amplitude of the jamming tone signal, and $\emptyset_J$ is the jamming signal phase with uniform distribution $\emptyset_J \sim (0,2\pi)$.

Fig. 2 shows the receiver block diagram for user 1, hop 1, FH frequency f_1, and symbol 1. The received output signal from the band-pass filter (BPF) is multiplied by a receiver post processing gain α_1 if a single antenna is employed or a receiver spatial domain beam-forming (SDBF) vector $\boldsymbol{\alpha} = (\alpha_1, \cdots, \alpha_{N_r})^T$ if N_r, number of multiple antennas, are used. We assume a single antenna receiver and Rician fading with channel efficient h_1, which can be estimated through the inserted pilot or reference symbols in a frame [19]-[22]. Then, we can set $\alpha_1 = a_1 e^{-j\theta_1}$ because of the available channel state information and can choose a_1 to maximize the received signal-to-jamming plus noise power ratio (SJNR) γ. The BPF and post-processing signal can be written as

$$r(t) = \left[h_1 s_{11}^{(1)}(t) + j_1(t) + n_1(t)\right]\alpha_1 = |h_1| a_1 s_{11}^{(1)}(t) + j_1(t) a_1 e^{-j\theta_1} + n_1(t) a_1 e^{-j\theta_1}. \quad (3)$$

Then, the received signal $r(t)$ is down-converted in frequency to in-phase (I) and quadrature-phase (Q) baseband signal components using two orthonormal basis functions, $\emptyset_1(t)$ and $\emptyset_2(t)$, and passed through the filters matched to the RRC waveform-shaping filter $g(t)$. Then, samples are taken of every symbol interval at each I and Q branch. In the rest of this paper without loss of generality, the subscripts used for user 1, symbol time 1, hop 1, and frequency f_1 are dropped. This is because we assume an independent symbol-by-symbol decision.

Let r_1 and r_2 denote I and Q branch samples, respectively for the user 1 signal. Let $\boldsymbol{r} = (r_1, r_2)^T$, $\boldsymbol{s} = (s_1, s_2)^T$, $\boldsymbol{j} = (j_1, j_2)^T$, and $\boldsymbol{n} = (n_1, n_2)^T$ denote the received signal, the transmitted signal component, the jamming signal component, and the noise component vector, respectively. Here, $r_i = \langle r(t), \emptyset_i(t) \rangle$ is an inner product of $r(t)$ and $\emptyset_i(t)$, which is the projection of the received signal into the base function $\emptyset_i(t)$, $i = 1,2$.

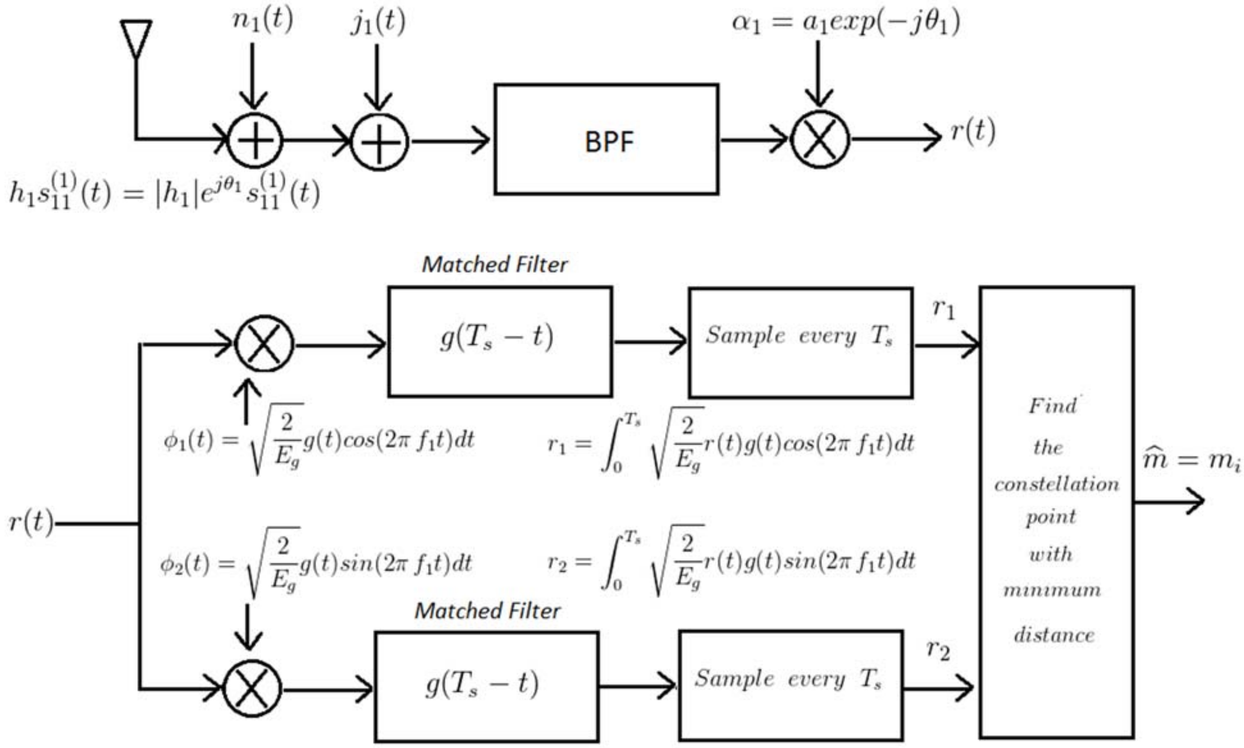

Figure 2. Receiver for user 1, hop 1, FH frequencyf_1, and symbol 1.

The received signal vector can be written as

$$\boldsymbol{r} = \begin{cases} |h_1| a_1 \boldsymbol{s} + a_1 \boldsymbol{j} + a_1 \boldsymbol{n} & if\ jammed \\ |h_1| a_1 \boldsymbol{s} + a_1 \boldsymbol{n} & if\ unjammed \end{cases}. \tag{4}$$

Hence, the received SJNR or signal-to-noise power ratio (SNR) γ, depending on the jamming conditions, can be written as

$$\gamma = \begin{cases} \frac{E[\| |h_1| a_1 \boldsymbol{s} \|^2]}{E[\| a_1 \boldsymbol{j} + a_1 \boldsymbol{n} \|^2]} = \frac{(|h_1| a_1)^2 P_S}{(a_1)^2 (P_J + P_N)} & if\ jammed \\ \frac{E[\| |h_1| a_1 \boldsymbol{s} \|^2]}{E[\| a_1 \boldsymbol{n} \|^2]} = \frac{(|h_1| a_1)^2 P_S}{(a_1)^2 P_N} & if\ unjammed \end{cases} \tag{5}$$

where $P_S = E[\|\boldsymbol{s}\|^2]$, $P_J = E[\|\boldsymbol{j}\|^2]$, and $P_N = E[\|\boldsymbol{n}\|^2]$ denote the signal component, the jamming component, and noise component powers, respectively. We assume in (5) that the jamming signal phase $\emptyset_J$ is equal to the desired signal phase for the worst case consideration. In addition, in (5) we assume the PBTJ as a PBNJ for simplification and the same jamming power is simply added to the AWGN power. By applying the Cauchy-Schwartz inequality to (5), (i.e., $|\langle \boldsymbol{x}, \boldsymbol{y} \rangle|^2 \leq \|\boldsymbol{x}\|^2 \|\boldsymbol{y}\|^2$ with "=" if and only if $\boldsymbol{x} = c\boldsymbol{y}$ for any constant c), the maximum γ can be achieved when a_1 is proportional to $|h_1|$. Hence, we choose a_1 as

$$a_1 = \begin{cases} \frac{|h_1|}{\sqrt{P_J + P_N}} & if\ jammed \\ \frac{|h_1|}{\sqrt{P_N}} & if\ unjammed. \end{cases} \tag{6}$$

Note that $(a_1)^2$ in (5) can directly cancel each other in the numerator and the denominator. However, when the receiver employs M_r number of multiple antennas, the terms $(|h_1|a_1)^2$ and $(a_1)^2$ used for the single-antenna case in the numerator and denominator of (5) will be changed to $\left(\sum_{i=1}^{M_r} |h_i| a_i\right)^2$ and $\sum_{i=1}^{M_r} a_i^2$, respectively. Therefore, the Cauchy-Schwartz inequality will be useful to determine the optimum weighting vector $\boldsymbol{a} = (a_1, \ \cdots, \ a_{M_r})^T$, which is proportional to the channel magnitude vector $\boldsymbol{h}_{mag} = \left(|h_1|, \ \cdots, \ |h_{M_r}|\right)^T$. Then, when the optimum weighting vector is used, the maximum instantaneous SJNR or maximum SNR can be written as

$$\gamma_{max} = \begin{cases} \frac{(|h_1|)^2 P_S}{(P_J + P_N)} & if\ jammed \\ \frac{(|h_1|)^2 P_S}{P_N} & if\ unjammed. \end{cases} \tag{7}$$

Here, the noise component power can be written as

$$P_N = N_0 B = N_0 / T_s. \tag{8}$$

This is because the signal channel bandwidth B is approximately equal to $1/T_s$. Let W denote the entire FH spectrum bandwidth. Then, $W = N_f B$. And the PBTJ power per tone can be written as

$$P_J = A_J^2 = \frac{P_{J,total}}{Number\ of\ PBTJ\ tones\ in\ W} = \frac{P_{J,total}}{\beta \frac{W}{B}} = \frac{N_J B}{\beta} = \frac{N_J}{\beta T_s} \tag{9}$$

where β denotes the jamming fraction ratio, $0 < \beta \leq 1$, and N_J denotes the equivalent jamming power spectral density, which is

$$N_J = \frac{P_{J,total}}{W}. \tag{10}$$

Assume a random FH pattern in this paper. Then, the jamming fraction ratio β is equal to the probability of a frequency tone being jammed. This is because

$$Pr(A\ signal\ tone\ is\ jammed\ by\ PBTJ\ ) = \frac{Number\ of\ Tones\ Jammed\ by\ PBTJ}{Total\ Number\ of\ Tones} = \frac{\beta\frac{W}{B}}{\frac{W}{B}} = \beta. \tag{11}$$

Hence, γ_{max} in (5) can be rewritten as

$$\gamma_{max} = \begin{cases} \frac{(|h_1|)^2 P_S}{\left(\frac{N_J}{\beta T_S}+N_0\frac{1}{T_S}\right)} = \frac{(|h_1|)^2 E_S}{\left(\frac{N_J}{\beta}+N_0\right)} = \frac{(|h_1|)^2}{\left(\frac{1}{\beta E_S/N_J}+\frac{1}{E_S/N_0}\right)} & if\ jammed\ with\ prob.\ \beta \\ \frac{(|h_1|)^2 P_S}{N_0\frac{1}{T_S}} = \frac{(|h_1|)^2 E_S}{N_0} & if\ unjammed\ with\ prob. (1-\beta). \end{cases} \tag{12}$$

The purpose of PBTJ is to minimize SJNR γ, whereas the purpose of receiver beam forming (BF) is to maximize γ. We can consider the min-max problem as

$$min_{\beta, 0<\beta\leq 1}\ max_{a_1 \geq 0} = \gamma(a_1, \beta). \tag{13}$$

3.1 EXACT SYMBOL ERROR RATE ANALYSIS

For a given instantaneous SNR or SJNR γ, the exact SER of FH MPSK under PBTJ and Rician fading can be obtained using Craig's formula in [25], [26] as

$$P_s(E|\gamma) = \frac{1}{\pi}\int_0^{(M-1)\pi/M} exp\left[\frac{-g\gamma}{sin^2\emptyset}\right] d\emptyset \tag{14}$$

where

$$g = sin^2\frac{\pi}{M}. \tag{15}$$

The average SER of FH MPSK over Rician fading and the jamming state random variable J can be written as

$$\bar{P}_s(E) = E_{\gamma,J}[P_s(E|\gamma,J)] = E_{\gamma_J}\left[P_s\left(E\middle|\gamma_J,J=1\right)\right]Pr[J=1] + E_{\gamma_N}[P_s(E|\gamma_N,J=0)]Pr[J=0] \quad (16)$$

where $J = 1$ and $J = 0$ denote the presence and absence of PBTJ, respectively, at the desired signal tone, hop, and symbol times of interest; hence, $Pr[J = 1]$ and $Pr[J = 0]$ would be β and $(1 - \beta)$, respectively. And the SJNR and SNR are written, respectively, as

$$\gamma_J = \frac{(|h_1|)^2}{\left(\frac{1}{\beta E_S/N_J}+\frac{1}{E_S/N_0}\right)} \quad (17)$$

and

$$\gamma_N = \frac{(|h_1|)^2 E_S}{N_0}. \quad (18)$$

Note that both γ_J and γ_N are Rician fading. Also,

$$E_{\gamma_J}\left[P_s\left(E\middle|\gamma_J,J=1\right)\right] = \int_0^\infty P_s\left(E\middle|\gamma_J,J=1\right)p_{\gamma_J}\left(\gamma_J\right)d\gamma_J$$

$$= \int_0^\infty \frac{1}{\pi}\int_0^{(M-1)\pi/M} exp\left[\frac{-g\gamma_J}{sin^2\emptyset}\right]d\emptyset\, p_{\gamma_J}\left(\gamma_J\right)d\gamma_J = \frac{1}{\pi}\int_0^{(M-1)\pi/M}\int_0^\infty exp\left[\frac{-g\gamma_J}{sin^2\emptyset}\right]p_{\gamma_J}\left(\gamma_J\right)d\gamma_J d\emptyset$$

$$= \frac{1}{\pi}\int_0^{(M-1)\pi/M}\int_0^\infty exp\left[\frac{-g\gamma_J}{sin^2\emptyset}\right]p_{\gamma_J}\left(\gamma_J\right)d\gamma_J d\emptyset = \frac{1}{\pi}\int_0^{(M-1)\pi/M} M_{\gamma_J}\left(\frac{-g}{sin^2\emptyset}\right)d\emptyset$$

$$= \frac{1}{\pi}\int_0^{(M-1)\pi/M}\frac{(1+K)}{(1+K)+\frac{g}{sin^2\emptyset}\bar{\gamma}_J}\exp\left[\frac{-K\frac{g}{sin^2\emptyset}\bar{\gamma}_J}{(1+K)+\frac{g}{sin^2\emptyset}\bar{\gamma}_J}\right]d\emptyset \quad (19)$$

where $M_{\gamma_J}(s)$ is the MGF of γ_J, i.e., $M_{\gamma_J}(s) = E_{\gamma_J}[e^{s\gamma_J}]$. From [24], [25], the MGFs for various fading environments can be written as follows:

a) For Rayleigh fading,

$$M_{\gamma_J}\left(\frac{-g}{sin^2\emptyset}\right) = \left(1+\frac{g\bar{\gamma}_J}{sin^2\emptyset}\right)^{-1}. \quad (20)$$

b) For Rician with factor K,

$$M_{\gamma_J}\left(\frac{-g}{sin^2\emptyset}\right) = \frac{(1+K)sin^2\emptyset}{(1+K)sin^2\emptyset+g\bar{\gamma}_J}\exp\left[\frac{-Kg\bar{\gamma}_J}{(1+K)sin^2\emptyset+g\bar{\gamma}_J}\right]. \quad (21)$$

c) For Nakagami-*m* fading,

$$M_{\gamma_J}\left(\frac{-g}{sin^2\emptyset}\right) = \left(1 + \frac{g\bar{\gamma}_J}{msin^2\emptyset}\right)^{-m}. \quad (22)$$

Our results are applicable for other modulations by modifying (14) and other fading environments by finding the corresponding MGF for the other fading. For example, the exact SER of a rectangular MQAM modulation can be written as

$$P_s(E|\gamma) = 1 - \left(1 - \frac{2(\sqrt{M}-1)}{\sqrt{M}} Q\left(\sqrt{3\gamma/(M-1)}\right)\right)^2 = 1 - \left(1 - \frac{2(\sqrt{M}-1)}{\sqrt{M}} \frac{1}{\pi} \int_0^{\pi/2} exp\left[\frac{-3\gamma/(M-1)}{2sin^2\emptyset}\right] d\emptyset\right)^2 \quad (23)$$

where γ is the instantaneous SNR under fading but the averaged SNR over all possible M-ary constellation points for a given fading coefficient. Substituting (23) into (14), we can find the exact SER of the FH MQAM under PBTJ plus Rician fading as we have done for the FH MPSK. Therefore, we present only the Rician fading and MPSK modulation case in the remainder of this paper.

In (19), we need to calculate the average SJNR $\bar{\gamma}_J$ over the Rician fading under the PBTJ condition as

$$\bar{\gamma}_J = E_{|h_1|^2}\left[\frac{(|h_1|)^2}{\left(\frac{1}{\beta E_S/N_J} + \frac{1}{E_S/N_0}\right)}\right] = \frac{1}{\left(\frac{1}{\beta E_S/N_J} + \frac{1}{E_S/N_0}\right)} E_{|h_1|^2}[|h_1|^2]. \quad (24)$$

The $E_{|h_1|^2}[|h_1|^2]$ can be computed using [9], [24], [25] as

$$E_{|h_1|^2}[|h_1|^2] = \sigma\sqrt{\pi/2}\, L_{1/2}(-s^2/2\sigma^2) = \sigma\sqrt{\pi/2}\, L_{1/2}(-K) \quad (25)$$

where $2\sigma^2$ is the non-line-of-sight (NLOS) component power, s^2 is the LOS component power, and $K = s^2/\,2\sigma^2$ is the ratio of the line-of-sight (LOS) over NLOS component power called the Rician factor. Here, the $L_{1/2}(x)$ is the Laguerre polynomial, written as

$$L_{1/2}(x) = e^{x/2}\left[(1-x)I_0\left(\frac{-x}{2}\right) - xI_1\left(\frac{-x}{2}\right)\right] \tag{26}$$

where $I_0(x)$ and $I_1(x)$ are the zeroth order and the first-order modified Bessel function of the first kind, respectively. Assume $\sigma^2 = 1$ without of loss of generality. Hence,

$$E_{|h_1|^2}[|h_1|^2] = \sigma\sqrt{\pi/2}\,L_{1/2}(-s^2/2\sigma^2) = \sqrt{\pi/2}\,L_{1/2}(-K)$$

$$= \sqrt{\pi/2}\,e^{-K/2}\left[(1+K)I_0\left(\frac{K}{2}\right) + KI_1\left(\frac{K}{2}\right)\right]. \tag{27}$$

$$\bar{\gamma}_J = \frac{1}{\left(\frac{1}{\beta E_S/N_J} + \frac{1}{E_S/N_0}\right)}\sqrt{\pi/2}\,e^{-K/2}\left[(1+K)I_0\left(\frac{K}{2}\right) + KI_1\left(\frac{K}{2}\right)\right]. \tag{28}$$

Substituting $\bar{\gamma}_J$ into (19), we can find an exact conditional SER of the FH MPSK given a PBTJ condition.

We repeat (19) to (28) to obtain the conditional average SER under no-jamming as

$$E_{\gamma_N}\left[P_s\left(E|\gamma_J, J=0\right)\right] = \int_0^\infty P_s(E|\gamma_N, J=0)p_{\gamma_N}(\gamma_N)d\gamma_N$$

$$= \frac{1}{\pi}\int_0^{(M-1)\pi/M} \frac{(1+K)}{(1+K)+\frac{g}{\sin^2\emptyset}\bar{\gamma}_N} \exp\left[\frac{-K\frac{g}{\sin^2\emptyset}\bar{\gamma}_N}{(1+K)+\frac{g}{\sin^2\emptyset}\bar{\gamma}_N}\right] d\emptyset \tag{29}$$

where

$$\bar{\gamma}_N = \frac{E_S}{N_0}\sqrt{\frac{\pi}{2}}\,e^{-K/2}\left[(1+K)I_0\left(\frac{K}{2}\right) + KI_1\left(\frac{K}{2}\right)\right]. \tag{30}$$

Therefore, the overall averaged exact SER of the FH MPSK under PBTJ and Rician fading can be written using (16), (19), and (28)–(30) as

$$\bar{P}_s(E|\beta) = \frac{1}{\pi}\int_0^{(M-1)\pi/M} \frac{(1+K)}{(1+K)+\frac{g}{\sin^2\emptyset}\bar{\gamma}_J} \exp\left[\frac{-K\frac{g}{\sin^2\emptyset}\bar{\gamma}_J}{(1+K)+\frac{g}{\sin^2\emptyset}\bar{\gamma}_J}\right] d\emptyset \cdot \beta$$

$$+ \frac{1}{\pi}\int_0^{(M-1)\pi/M} \frac{(1+K)}{(1+K)+\frac{g}{\sin^2\emptyset}\bar{\gamma}_N} \exp\left[\frac{-K\frac{g}{\sin^2\emptyset}\bar{\gamma}_N}{(1+K)+\frac{g}{\sin^2\emptyset}\bar{\gamma}_N}\right] d\emptyset \cdot (1-\beta) \tag{31}$$

The average SER for a given jamming fraction ratio β can be rewritten by substituting (28) and (30) into (31) as

$$\bar{P}_s(E|\beta) = \frac{1}{\pi}\int_0^{(M-1)\pi/M}\left[\frac{\beta(1+K)}{(1+K)+\frac{g}{sin^2\emptyset}\frac{1}{\left(\frac{1}{\beta E_S/N_J}+\frac{1}{E_S/N_0}\right)}\sqrt{\pi/2}e^{-\frac{K}{2}}\left[(1+K)I_0\left(\frac{K}{2}\right)+KI_1\left(\frac{K}{2}\right)\right]}\right.$$

$$\left.\cdot \exp\left(\frac{-K\frac{g}{sin^2\emptyset}\frac{1}{\left(\frac{1}{\beta E_S/N_J}+\frac{1}{E_S/N_0}\right)}\sqrt{\pi/2}e^{-\frac{K}{2}}\left[(1+K)I_0\left(\frac{K}{2}\right)+KI_1\left(\frac{K}{2}\right)\right]}{(1+K)+\frac{g}{sin^2\emptyset}\frac{1}{\left(\frac{1}{\beta E_S/N_J}+\frac{1}{E_S/N_0}\right)}\sqrt{\pi/2}e^{-\frac{K}{2}}\left[(1+K)I_0\left(\frac{K}{2}\right)+KI_1\left(\frac{K}{2}\right)\right]}\right)\right]d\emptyset$$

$$+\frac{1}{\pi}\int_0^{(M-1)\pi/M}\frac{(1-\beta)(1+K)}{(1+K)+\frac{g}{sin^2\emptyset}\bar{\gamma}_N}\exp\left[\frac{-K\frac{g}{sin^2\emptyset}\bar{\gamma}_N}{(1+K)+\frac{g}{sin^2\emptyset}\bar{\gamma}_N}\right]d\emptyset. \quad (32)$$

The averaged bit error rate of the FH MPSK under PBTJ and Rician fading for a given jamming fraction ratio β can be obtained using (32) as

$$\bar{P}_b(E|\beta) \approx \frac{1}{log_2(M)}\bar{P}_s(E|\beta). \quad (33)$$

Here, we assume Gray encoding so that the neighbor signal constellations are only one bit different from the desired symbol constellation point.

For a special case, consider only AWGN and PBTJ. Then, the Rician factor K becomes ∞. So, the exact SER of the FH MPSK under AWGN and PBTJ can be written as

$$P_s(E|\beta) = \frac{1}{\pi}\int_0^{(M-1)\pi/M}\exp\left[-\frac{g}{sin^2\emptyset}\gamma_N\right]d\emptyset\cdot(1-\beta)+\frac{1}{\pi}\int_0^{(M-1)\pi/M}\exp\left[-\frac{g}{sin^2\emptyset}\gamma_J\right]d\emptyset\cdot\beta \quad (34)$$

where SNR $\gamma_N = E_S/N_0$ and SJNR $\gamma_J = \frac{1}{\left(\frac{1}{\beta E_S/N_J}+\frac{1}{E_S/N_0}\right)}$ from (12). Thus, the first and second terms of (34) represent the exact SER when the signal is not jammed with probability $(1-\beta)$ and jammed with probability β, respectively.

3.2 OPTIMAL TONE-JAMMING FRACTION

The optimal jamming fraction β, which maximizes the average conditional SER $\bar{P}_s(E|\beta)$, can be numerically found by taking the derivative of (32) with respect to β for a given set of parameters, such as E_S/N_J, E_S/N_0, and M, and Rician fading factor K. The optimal β should satisfy the following equation:

$$\frac{1}{\pi}\int_0^{(M-1)\pi/M}\frac{(1+K)}{(1+K)+\frac{g}{sin^2\emptyset}\bar{\gamma}_N}\exp\left[\frac{-K\frac{g}{sin^2\emptyset}\bar{\gamma}_N}{(1+K)+\frac{g}{sin^2\emptyset}\bar{\gamma}_N}\right]\,d\emptyset$$

$$=\frac{1}{\pi}\int_0^{(M-1)\pi/M}\left[\frac{-g\bar{\gamma}_J N_J sin^2\emptyset(1+K)}{\beta(1+K)sin^2\emptyset+g\bar{\gamma}_J\beta}+\exp\left(\frac{-Kg\bar{\gamma}_J}{(1+K)sin^2\emptyset+g\bar{\gamma}_J}\right)\right.$$

$$\left.\cdot\frac{g\bar{\gamma}_J\cdot sin^2\emptyset\cdot(1+K)\left(N_0K+\frac{\beta-K}{\beta}\right)+(1+K)^2\cdot sin^4\emptyset\cdot\left(N_0\beta+N_J\right)}{g\bar{\gamma}_J+(1+K)\cdot sin^2\emptyset}\right]d\emptyset. \quad (35)$$

The left term of (35) is the derivative of the second term on the right-hand side of (32), and the right term of (35) is the derivative of the first term on the right-hand side of (32). Using Newton's method, we can solve the optimal beta using (35).

4.0 NUMERICAL RESULTS AND DISCUSSION

Figure 3 shows BER versus E_s/N_0 with PBTJ fraction β in percentile as a parameter for a given $E_s/N_J = 5\ dB$, given small Rician factor $K = 0.1$, and given quadrature hse shift keying (QPSK) modulation. Observe that when there is no jamming, the BER curve is close to the BER of Rayleigh fading. This is because Rician factor is small; $K = 0.1$. Also observe that the optimum (i.e., worst) jamming fraction is 100 percentile.

Figure 4 shows the BER versus E_s/N_0 in dB for QPSK under Rician of factor $K = 0.9$, $E_s/N_J = 10\ dB$, PBTJ fraction $\beta = 0.1$ with MPSK as a parameter. Observe that even the jamming power spectral density is 10 dB smaller than the symbol energy as $E_s/N_J = 10\ dB$, the BER is unacceptably high for all modulations.

Figure 5 shows the BER versus PBTJ fraction β for binary phase shift keying (BPSK) under Rician fading of factor $K = 0.1$, $E_b/N_0 = 10\ dB$ with E_b/N_J as a parameter in dB. Observe that the optimum fraction β is 1 for all E_b/N_J. This is an interesting result. If the LOS is small, then the channel becomes almost completely subject to Rayleigh fading. Then, the worst jamming fraction is 1. If the PBTJ jammer is aware that the communicators are under a Rayleigh fading environment, he would use a broadband jamming strategy.

Figure 6 shows the corresponding BER versus PBTJ fraction β for BPSK under Rician fading of a strong LOS component case with $K = 5$, using (32) and (33), $E_b/N_0 = 10\ dB$ with E_b/N_J as a parameter in dB. Observe that the optimum jamming fraction can be less than 1 when E_b/N_J is high. For example, the PBTJ has an insufficient jamming power such as $E_b/N_J = 5\ dB$, the optimum jamming fraction is 0.1.

Figure 7 also shows BER versus PBTJ jamming fraction β with E_S/N_J as a parameter, using (34) for no fading but under AWGN and PBTJ, for a given $E_b/N_0 = 10\ dB$ and for BPSK modulation. Again, observe that the optimum jamming fraction can be less than 1 when E_b/N_J is high, i.e., the total available jamming power is insufficient. For example, if the PBTJ has an insufficient jamming power such as $E_b/N_J = 5\ dB$, the optimum jamming fraction is 0.3.

An important observation can be made in Figs. 3 to 5 that when NLOS is dominant, e.g., Rician factor K is very small such as 0.1 or 0.9, the fading channel becomes Rayleigh dominated, and the BER worsens as the PBTJ fraction β increases. Thus, the optimum jamming fraction would be 1. In other words, wideband PBTJ is more effective against the desired user than narrowband PBTJ. This may be because when there is no LOS or weak LOS components in the fading, the received signal spectrum can be more spread over in the signal bandwidth than a Rician fading channel of a strong factor.

However, as shown in Figs. 6 to 7, when no fading but only AWGN and PBTJ are present in the system (in other words only the LOS component is present with $K = \infty$), or with Rician fading of a strong LOS component having $K = 5$, the optimum PBTJ jamming fraction becomes smaller than 1 as E_b/N_J increases (i.e., as jamming power gets weaker). For example, the optimum beta is around 0.3 in Fig. 7 when $E_b/N_J = 5\ dB$, $E_b/N_0 = 10\ dB$, and BPSK is used with no fading. And the optimum beta decreases from 0.3 to 0.08 when E_b/N_J increases from $5\ dB$ to $10\ dB$. Hence, a narrower PBTJ would be more effective than a wider PBTJ when the jamming power gets weaker for the AWGN or for the AWGN plus Rician fading of a strong LOS component such as $K = 5$ and PBTJ channel. The optimum beta shown in Fig. 7 agrees with those obtained through numerical searches using (35).

These observations can be useful in the game-theoretic, protected, tactical waveform design [19]-[22]. For example, when a soldier is located in an NLOS environment, then the jammer is likely to use a broad band jamming signal, whereas when a soldier is placed in a strong LOS environment, then the jammer is likely to employ a narrow band jamming, depending on his available jamming power. Using this hypothesis, we may design a strategically more effective FH pattern. For example, when a jammer employs a narrow band jamming, then a random FH pattern is not the best strategy in the SER performance perspective although the random FH pattern can show a low probability of detection. If a probability of a certain tone frequency being jammed is high, then a smart FH pattern generator can avoid that tone and use the FH tones of less probability being jammed more frequently.

Finally, Figs. 8 and 9 show BER versus E_b/N_0 SNR in dB for BPSK under Rician fading with $K = 0.1$ (weak) and $K = 10$ (strong) LOS components, respectively. Here, the number of receiver BF antennas ($N_r = 1, 10, 100$) is a parameter, and the PBTJ fraction ($\beta = 0.5$) and

$E_b/N_J = 5\ dB$ are assumed. Observe that the BER performance can be improved significantly when the receiver employs multiple antenna elements for the BF purpose. Rationale for this significant receiver BF gain can be stated as follows: The average received SJNR $\bar{\gamma}_J$ under the fading and jamming environment in (24) and the average received SNR $\bar{\gamma}_N$ under fading and AWGN become, respectively,

$$\bar{\gamma}_J = \frac{N_r}{\left(\frac{1}{\beta E_S/N_J} + \frac{1}{E_S/N_0}\right)} E_{|h_1|^2}[|h_1|^2] \quad (36)$$

and

$$\bar{\gamma}_N = N_r(E_S/N_0)E_{|h_1|^2}[|h_1|^2] \quad (37)$$

when a receiver employs N_r (number of) receiver BF antennas. Here, h_1 is the Rician multipath fading coefficient at the first antenna; the fading coefficients received at all antenna elements are independent and identically distributed when the antenna elements are separated with sufficiently large distance, e.g., larger than a half wavelength, and maximum ratio combing (MRC) is used at the receiver [25, Chapter 7]. This is called the diversity gain. The averaged SJNR $\bar{\gamma}_J$ and SNR $\bar{\gamma}_N$ under jamming and no jamming in (36) and (37) are used in (31) and (32), respectively, for the exact calculation of the average SER for a given jamming fraction ratio β. The results are plotted in Figs. 8 and 9 for two different Rician fadings with ($K = 0.1$) weak and ($K = 10$) strong LOS components under the 50% partial band tone jamming fraction ratio.

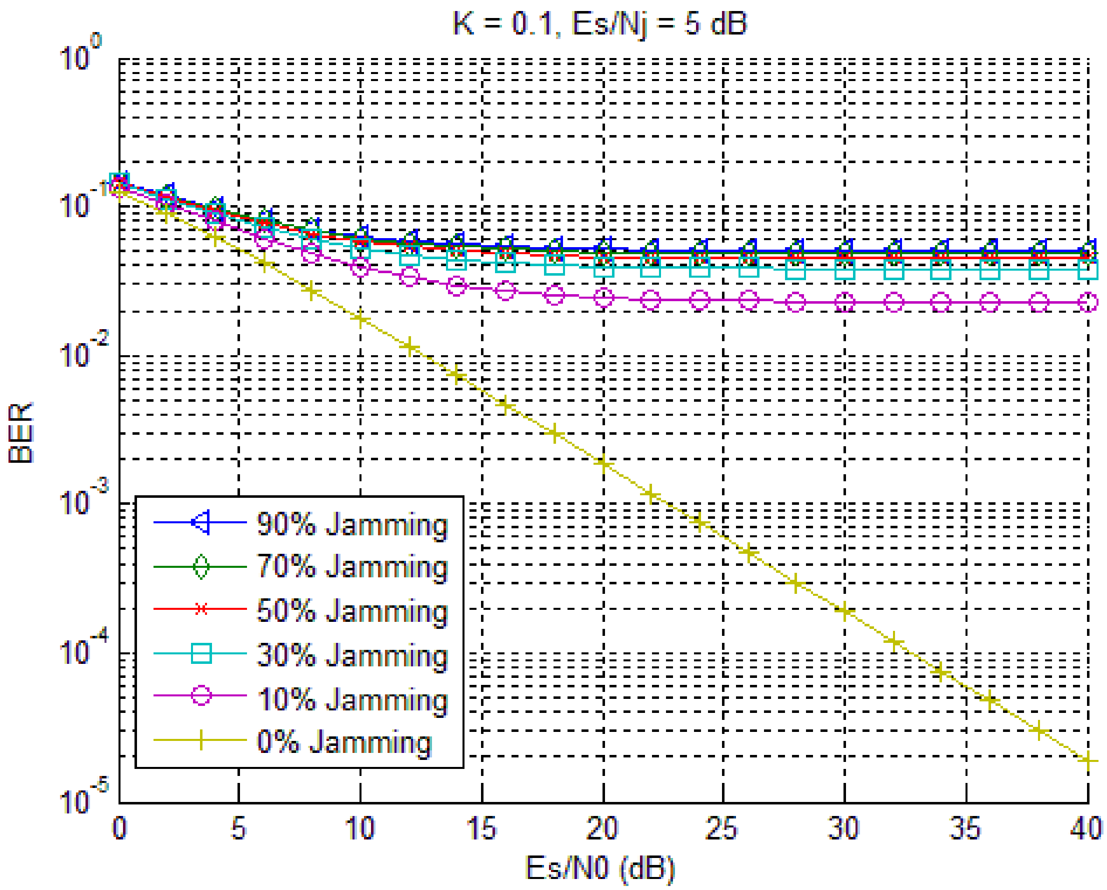

Figure 3. BER versus E_s/N_0 in dB for QPSK under Rician of factor $K = 0.1$, $E_s/N_J = 5\ dB$ with PBTJ fraction β in percentile as a parameter.

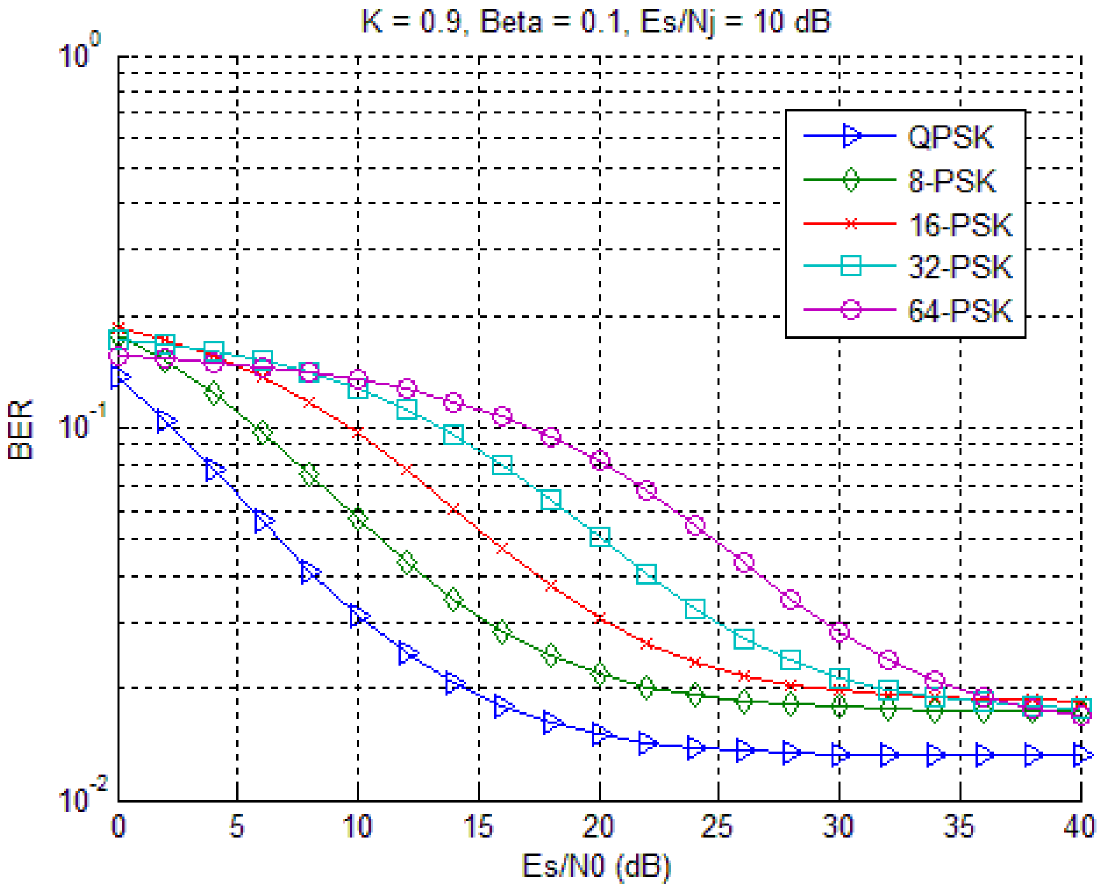

Figure 4. BER versus E_s/N_0 in dB for QPSK under Rician of factor $K = 0.9$, $E_s/N_J = 10\ dB$, PBTJ fraction $\beta = 0.1$ with MPSK as a parameter.

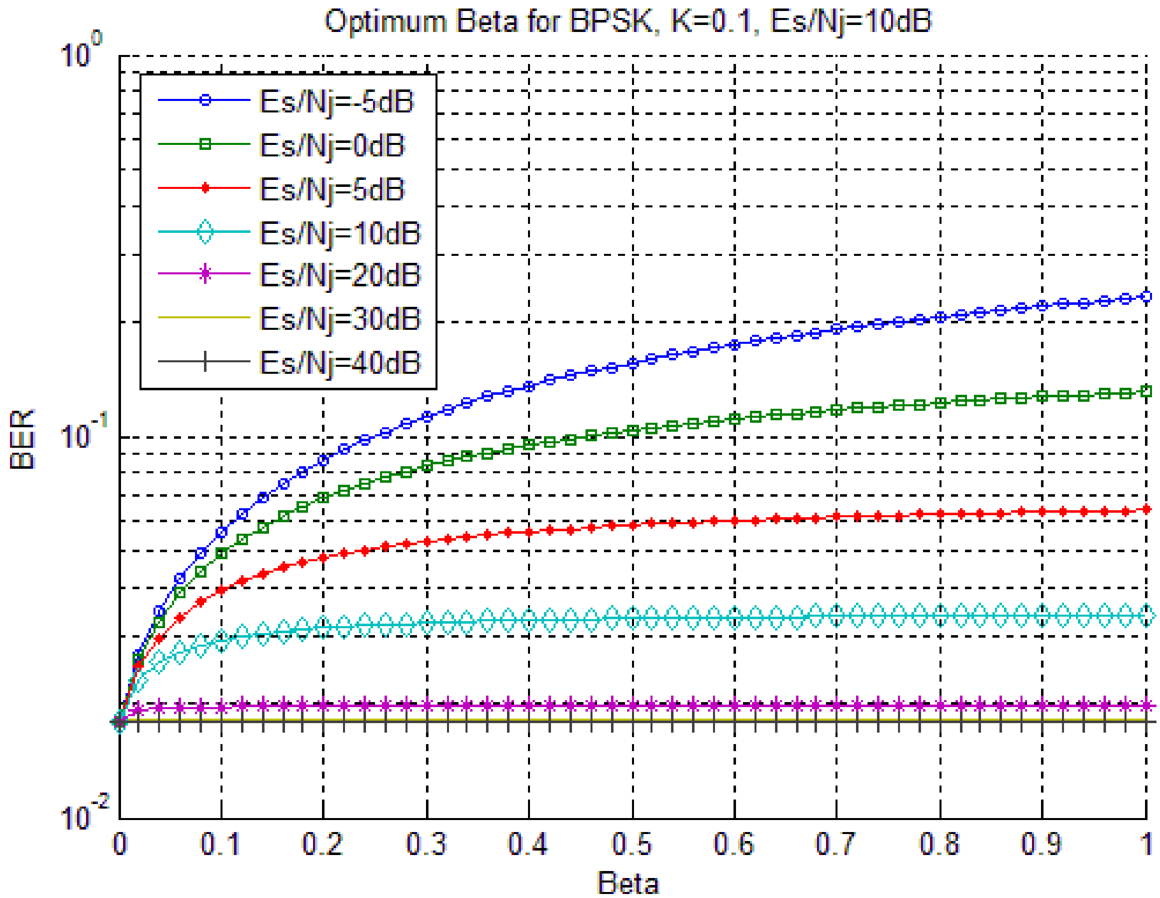

Figure 5. BER versus PBTJ fraction β for BPSK under Rician fading of factor $K = 0.1$, $E_b/N_0 = 10\ dB$ with E_b/N_J as a parameter in dB.

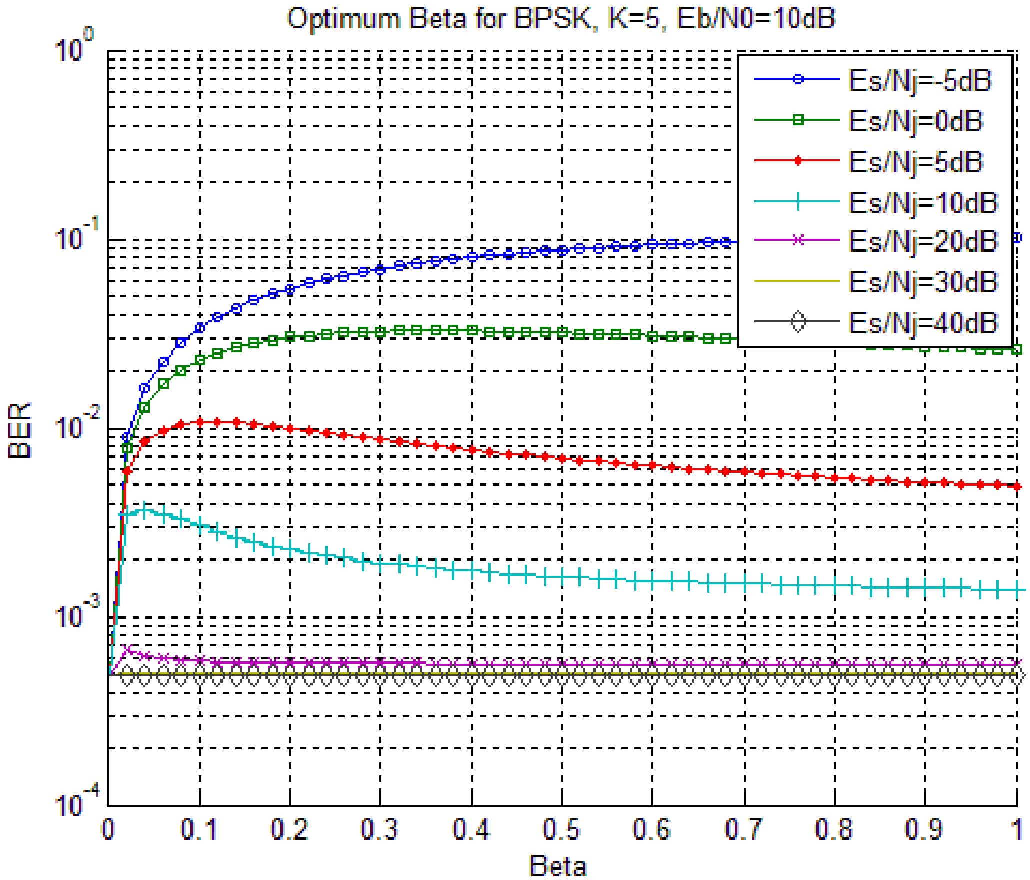

Figure 6. BER versus PBTJ fraction β for BPSK under Rician fading of factor $K = 5$, $E_b/N_0 = 10\ dB$ with E_b/N_J as a parameter in dB.

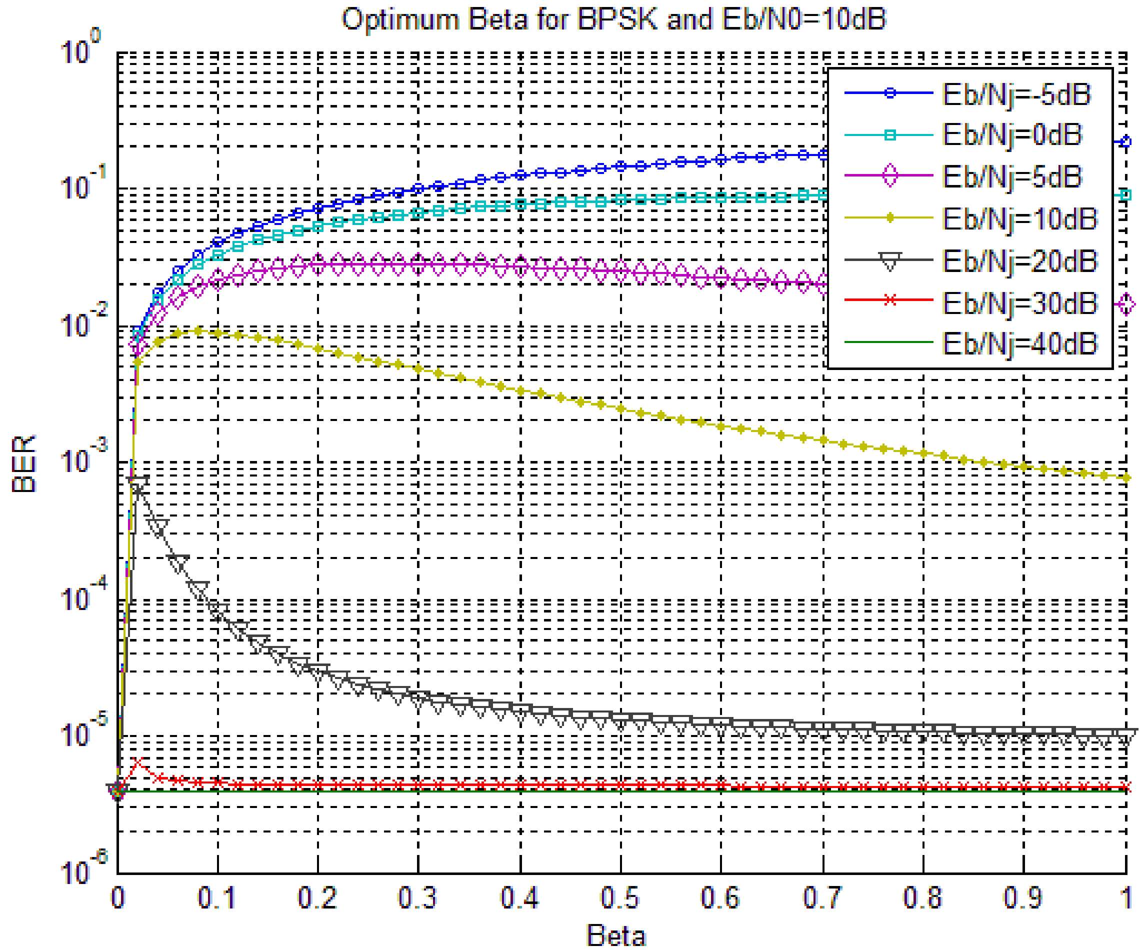

Figure 7. BER versus PBTJ fraction β for BPSK under no fading and $E_b/N_0 = 10\ dB$ with E_b/N_J as a parameter in dB.

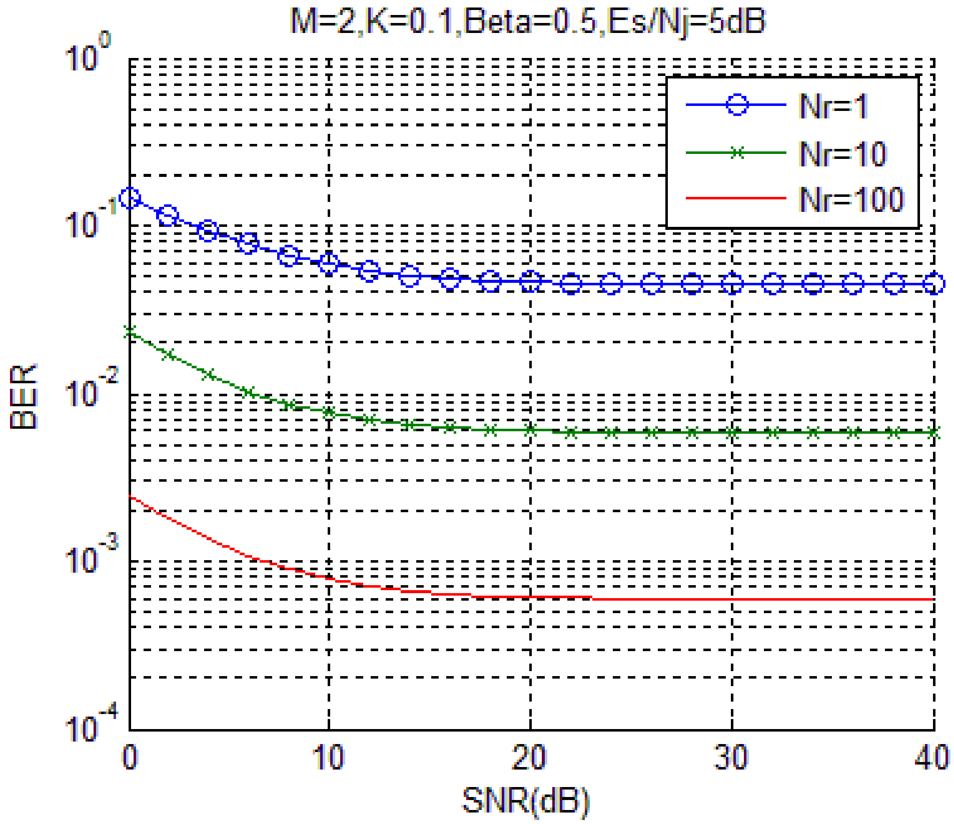

Figure 8. BER versus E_b/N_0 SNR in dB for BPSK under Rician fading with factor $K = 0.1$ weak LOS component, PBTJ fraction $\beta = 0.5$, $E_b/N_J = 5$ dB, and the number of receiver BF antennas ($N_r = 1, 10, 100$) as a parameter.

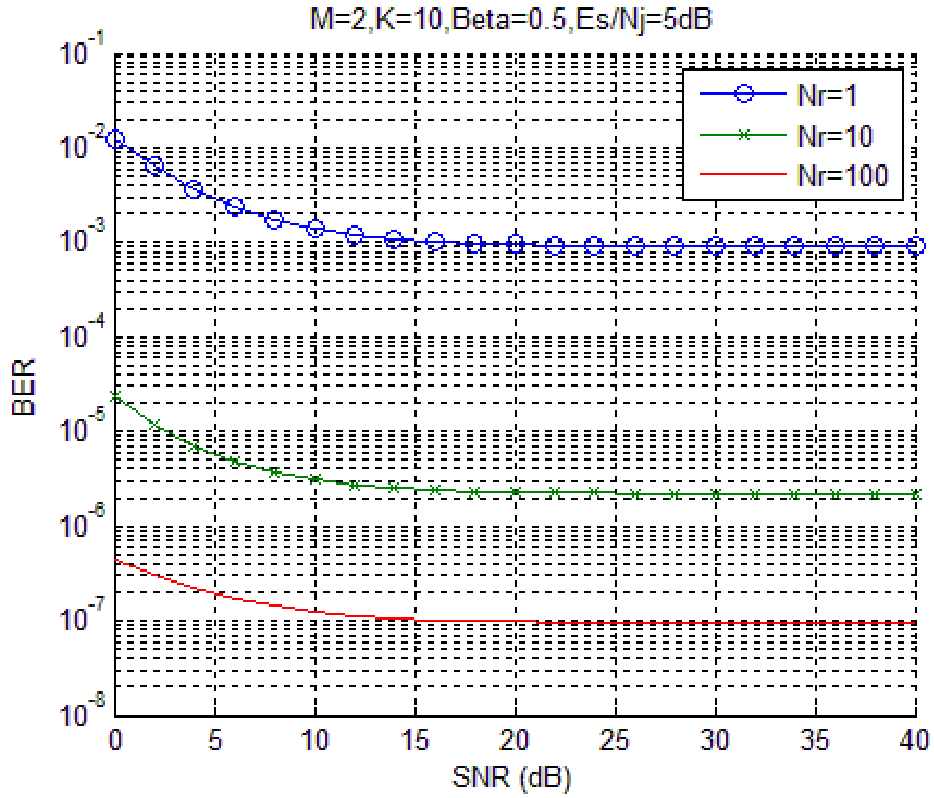

Figure 9. BER versus E_b/N_0 SNR in dB for BPSK under Rician fading with factor $K = 10$ strong LOS component, PBTJ fraction $\beta = 0.5$, $E_b/N_J = 5$ dB, and the number of receiver BF antennas $N_r = 1, 10, 100$ as a parameter.

5.0 Conclusions

We derived an exact symbol error rate expression for the FH system under partial-band tone jamming and Rician fading environments. The expression can be easily extended to other fading environments such as Rayleigh and Nakagami and other modulations such as MQAM. In addition, we studied the optimal weighting coefficients, called beamforming coefficients, to minimize the SER when channel coefficients are available. Furthermore, we presented an implicit expression of the worst PBTJ fraction ratio, which maximizes the SER of the FH system, and verified that the analytically derived optimal PBTJ fraction ratio agrees with those obtained through numerical computations. It was found that when the NLOS component in Rician fading is stronger than the LOS component, in other words when Rician factor K is small such as between 0.1 and 0.9, the worst PBTJ fraction ratio is 1. On the other hand, when Rician factor K gets larger than 1 and jamming power weakens, the optimum jamming fraction can be smaller than 1. For this case, narrowband PBTJ is more effective than wideband PBTJ. Results and observations in this paper would be useful in designing a future, efficient protected tactical waveform FH satellite and mobile communications system under PBTJ and fading or no-fading environments.

References

[1] M. Usuda, Y. Ishikawa, S. Onoe, "Optimizing the number of dedicated pilot symbols for forward link in W-CDMA systems," *Proceedings of Vehicular Technology Conference 2000*, Tokyo, Japan, vol. 3, pp. 2118–2122, May 2000.

[2] R. Love, A. Ghosh, W. Xiao, and R. Ratasuk, "Performance of 3GPP high speed downlink packet access (HSDPA)," IEEE 60th Vehicular Technology Conference, VTC2004-Fall, Los Angeles, CA, vol. 5, pp. 3359–3363, Sept. 2004.

[3] S. Abeta, "Toward LTE commercial launch and future plan for LTE enhancements (LTE-Advanced)," IEEE International Conference on Communication Systems (ICCS), Singapore, pp. 146–150, Nov. 2010.

[4] K.S. Gong, "Performance of Diversity Combining Techniques for FH/MFSK in Worst Case Partial Band Noise and Multi-Tone Jamming," IEEE Military Communications Conference, MILCOM 1983, Washington, D. C., vol. 1, pp. 17–21, Oct. 1983.

[5] R. Viswanathan and K. Taghizadeh, "Diversity combining in FH/BFSK systems to combat partial band jamming," *IEEE Transactions on Communications*, vol. 36, no. 9, pp. 1062–1069, Sept. 1988.

[6] C. Popper, M. Strasser, and, S. Capkun, "Anti-jamming broadcast communication using uncoordinated spread spectrum techniques," *IEEE Journal on Selected Areas in Communications*, vol. 28, no. 5, pp. 703–715, June 2010.

[7] J. H. Jr., Gass, and M. B. Pursley, "A comparison of slow-frequency-hop and direct-sequence spread-spectrum communications over frequency-selective fading channels," *IEEE Transactions on Communications*, vol. 47, no. 5, pp. 732–741, May 1999.

[8] P. Flikkema, "Spread-spectrum techniques for wireless communication," *IEEE Signal Processing Magazine*, vol. 14, no. 3, pp. 26–36, May 1997.

[9] Don Torrieri, *Principles of Spread-Spectrum Communication Systems*, 3rd ed., Springer, 2015.

[10] W. R. Fried, "Principles and Simulation of JTIDS Relative Navigation," *IEEE Transactions on Aerospace and Electronic Systems*, vol. AES-14, no. 1, pp. 76–84, Jan. 1978.

[11] R. Sabatini, L. Aulanier, H. Rutz, M. Martinez, L. Foreman, B. Pour, and S. Snow, "Multifunctional information distribution system (MIDS) integration programs and future developments," IEEE Military Communications Conference, MILCOM 2009, Boston, MA, pp. 1–7, Oct. 2009.

[12] J. Andrusenko, R. L. Miller, J. A. Abrahamson, N. M. Merheb Emanuelli, R. S. Pattay, and R. M. Shuford, "VHF General Urban Path Loss Model for Short Range Ground-to-Ground Communications," *IEEE Transactions on Antennas and Propagation*, vol. 56, no. 10, pp. 3302–3310, Oct. 2008.

[13] J. M. Rodriguez Bejarano, A. Yun, and B. De La Cuesta, "Security in IP satellite networks: COMSEC and TRANSEC integration aspects," Advanced Satellite Multimedia Systems Conference (ASMS) and 12th Signal Processing for Space Communications Workshop (SPSC), Baiona, Spain, pp. 281–288, Sept. 2012.

[14] M. B. Pursley and H. B. Russell, "Adaptive forwarding in frequency-hop spread-spectrum packet radio networks with partial-band jamming," *IEEE Transactions on Communications*, vol. 41, no. 4, pp. 613–620, Apr. 1993.

[15] Su Chun-Meng and L. B. Milstein, "Analysis of a coherent frequency-hopped spread-spectrum receiver in the presence of jamming," *IEEE Transactions on Communications*, vol. 38, no. 5, pp. 715–726, May 1990.

[16] Y. A. Chau and L. J. Mason, "Error probability for FH/MDPSK in multitone jamming, fast Rician fading, and Gaussian noise," *IEEE Transactions on Communications*, vol. 43, no. 2/3/4, pp. 545–553, Feb./Mar./Apr. 1995.

[17] Y. A. Chau, "Optimal partial decision diversity for frequency-hopped satellite communications in shadowed Rician fading channel with partial-band jamming," *Proceedings of IEEE 1993 Region 10 Conference Computer, Communication, Control and Power Engineering, TENCON '93*, Beijing, China, vol. 3, pp. 123–126, Oct. 19–21, 1993.

[18] D. J. Torrieri, "Fundamental limitations on repeater jamming of frequency-hopping communications," *IEEE J. Select. Areas Commun.*, vol. 7, no. 5, pp. 569–578, May 1989.

[19] Brian J. Wolf and Jacob C. Huang, "Implementation and Testing of the Protected Tactical Waveform (PTW)," IEEE Military Communications Conference, Tampa, FL, October 25–28, 2015.

[20] Thomas C. Royster and James Streitman, "Performance Considerations for Protected Wideband Satcom," IEEE Military Communications Conference, Tampa, FL, October 25–28, 2015.

[21] M. Glaser, K. Greiner, B. Hilburn, J. Justus, C. Walsh, W. Dallas, J. Vanderpoorten, and Jo-Chieh Chuang, "Protected MILSATCOM design for affordability risk reduction (DFARR)," IEEE Military Communications Conference, San Diego, CA, November 18–20, 2013.

[22] K. L. B. Cook, “Current wideband MILSATCOM infrastructure and the future of bandwidth availability,” *IEEE Aerospace and Electronics Systems Magazine*, pp. 23–28, 2008.

[23] M. K. Simon and M. S. Alouini, *Digital Communication over Fading Channels*, 2nd ed., Wiley-IEEE Press, December 6, 2004.

[24] M. K. Simon and M.S. Alouini, “A unified approach to the performance analysis of digital communications over generalized fading channels,” *IEEE Proceedings*, pp. 1860–1877, Sept. 1998.

[25] A. Goldsmith, *Wireless Communication*, 5th ed., Cambridge University Press, 2012.

[26] J. Craig, “New, simple, exact result for calculating probability of error for two-dimensional signal constellations,” *Proceedings Military Communications Conference*, McLean, Virginia, pp. 25.51–25.5.5, Nov. 1991.

[27] D. Torrieri, S. Cheng, M. C. Valenti, “Robust frequency hopping for interference and fading channels,” *IEEE Trans. Communications*, vol. 56, no. 8, pp. 1343–1351, Aug. 2008.

[28] G. Caire, G. Taricco, and E. Biglieri, “Bit-interleaved coded modulation,” *IEEE Trans. Inform. Theory*, vol. 44, pp. 927–946, May 1998.

[29] D. Torrieri, A. Mukherjee, and H. M. Kwon, “Coded DS-CDMA systems with iterative channel estimation and no pilot symbols,” *IEEE Trans. Wireless Commun.*, vol. 9, pp. 212–2021, June 2010.

LIST OF ACRONYMS AND ABBREVIATIONS

AF: amplify-and-forward

AWGN: additive white Gaussian noise

BER: bit error rate

BF: beamforming

β: partial-band tone jamming fraction

BPF: band-pass filter

BPSK: binary-phase-shift keying

dB: decibel

E_b/N_J: bit-energy-to-jamming power spectral density ratio

E_s/N_J: symbol-energy-to-jamming power spectral density ratio

E_s/N_0: symbol-energy-to-noise power spectral density ratio

FH: frequency-hopping

FHSS: frequency-hopping spread-spectrum

HSDPA: high-speed downlink packet access

I: in-phase

JTIDS: joint tactical information distribution system

K: Rician fading factor

L_h: the number of time hops per frame

LOS: line-of-sight

LTE: long-term evolution

MA: multiple access

MDPSK: M-ary differential phase-shift keying

MFSK: M-ary frequency-shift keying

MGF: moment generating function

MIDS: multifunctional information distribution system

MPSK: M-ary phase-shift keying

MQAM: M-ary quadrature amplitude-shift keying

MRC: maximum ratio combining

N_f: the total number of frequency positions in the entire hopping spectrum

N_J: jamming power spectral density ratio

N_r: the number of receiver antennas

N_s: the number of symbols transmitted per hop

N_u: the number o

NLOS: non-line-of-sight

PBNJ: partial-band noise jamming

PBTJ: partial-band tone jamming

Q: quadrature-phase

QPSK: quadrature-phase-shift keying

RRC: root-raised cosine filter

SC: system controller

SDBF: spatial domain beam-forming

SER: symbol error rate

SINCGARS: single-channel ground and airborne radio system

SIMO: single input multiple output

SISO: single input single output

SJNR: signal-to-jamming plus noise power ratio

SNR: signal-to-noise power spectral density ratio

SS: spread spectrum

T_h: a hopping time interval

TRANSEC: transmission security

W-CDMA: wideband-code division multiple access

DISTRIBUTION LIST

DTIC/OCP 8725 John J. Kingman Rd, Suite 0944 Ft Belvoir, VA 22060-6218	1 cy
AFRL/RVIL Kirtland AFB, NM 87117-5776	2 cys
Official Record Copy AFRL/RVSW/Khanh Pham	1 cy

(This page intentionally left blank)